CHANDRA
X-ray Center   60 Garden St., Cambridge Massachusetts 02138 USA

MEMORANDUM

1   Aimpoint and Optical Axis

We define the following two points in the Chandra focal plane (for more details, see Ref [1]):

- **Aimpoint:** Point where the image of an onaxis source with zero Y and Z offsets is located.

- **Optical Axis:** Point where the sharpest PSF is located.

The aimpoint and optical axis are close but not at the same point. Their relative positions are changing constantly. The positions on each detector and default offset are critical for the optimal operation of the Chandra X-ray Observatory.

2   Chandra Detectors and Aimpoints

Figure 1 shows the Chandra detectors layout in the Science Instrument Module (SIM) translation table. The SIM translation stage can move in the Z direction to place any one of the four detectors in the Chandra aimpoint for observation. The $\otimes$ on each detector marks the aimpoint position with zero pointing offset.

3   Aimpoint drift

The aimpoint of each individual observation can be derived by using the CIAO tool *dmcoords*, with the *evt2* & *asol* files and the pointing RA & Dec as the input. Subtracting the Y and Z offset (default or customized) from the above result, the aimpoint of zero offset for each observation can be obtained.

The Aimpoint has been drifting since the Chandra launch. Figures 2–5 show the aimpoint (with zero offset) positions of all the Chandra observations with nominal SIM-Z positions on all four detectors in chip coordinates as a function of time in the past 12 years of operation. The corresponding SIM Y and Z directions are also indicated next to the chip coordinates. The +'s in the figures mark the aimpoints of individual observations. The solid blue lines indicate the drift of median aimpoints in 6 months bins. It is seen that the aimpoint is drifting in both SIM $-$Y and $-$Z directions from 1999 until the beginning of year 2011. It is also seen that its short term fluctuation is also gradually increasing. The two sudden large jumps in June 2003 and November 2006 are due to the Aspect Camera Assembly (ACA) cooldown.

Since the beginning of 2011, the aimpoint has reversed its direction of drift, especially after the Safemode in July 2011. Figures 6–9 show the aimpoint positions since the beginning of 2010. It is seen that the aimpoint drifted further back (towards the positions of earlier years) after the safemode.

4 Optical Axis on HRC-I

The optical axis position is derived using the annual Ar Lac raster scan observations with HRC-I. The raster scan is a set of 21 observations of Ar Lac with two dimensional symmetrical offset with respect to the center (zero offset). The optical axis is found by fitting the encircled energy of each image in SKY coordinates as a function of the CHIP coordinates to a 2-dimensional quadratic function. The optical axis is located, by definition, at the CHIP position where the quadratic function is at its minimum. For details, see Ref [1].

Figure 10 shows 17 of the 21 AR Lac raster scan data points taken in September 2011 on HRC-I. Figure 11 shows the optical axis derived from the above data using the 2-D quadratic fit. The raster scan is taken every year, usually in September, so we can monitor the optical axis position. Figure 12 shows all the optical axis positions on HRC-I since launch. It moves like a random walk but is relatively stable. Its movement is well within a $10''$ region.

5 Optical Axis on HRC-S, ACIS-I and ACIS-S

In fact Figure 12 shows the pattern of optical axis movement in the focal plane, with the HRC-I coordinates while HRC-I is in its nominal SIM-Z position. When other detectors are in their nominal SIM-Z positions, the movement of the optical axis should be the same but registered with other detectors' coordinates.

Using *dmcoords*, one can transfer the coordinate position from one detector to another by setting the designated detector's name and its nominal SIM-Z position as the input. However, *dmcoords* is not perfect when performing this transfer. There is a small systematic error for each transfer, which needs to be corrected. These corrections can be calculated by transferring the aimpoints, as plotted in Figures 2–5, between the four detectors and comparing the transferred aimpoints with the actually observed aimpoints on that detector.

Figures 13–16 show the aimpoints transferred between the four detectors, using the nominal SIM-Z positions listed in Table 1. The colored dots in the figures are individual aimpoints transferred by *dmcoords*. The corresponding colored solid lines are the median aimpoint in 6 months bins. Had *dmcoords* done a perfect job, the four colored lines would have been stacked on top of each other. The fact they are not indicates there is a systematic offset. The gaps between the colored lines are the offsets need to be corrected. Since we want to know the optical axis position on detectors other than HRC-I, only the offset corrections for transferring from HRC-I to other three detectors are needed here. Table 2 lists the median, mean and $1 - \sigma$ standard deviation of the systematic offsets between the HRC-I and other three detectors. We use the median value for the correction, i.e. after transferring the optical axis coordinates from HRC-I to other detectors, the value in column "Median" is added to the transferred Chip X and Y coordinates to obtain more accurately determined positions.

Table 1: Nominal SIM-Z Positions

Detector	Nominal Sim-Z (mm)
ACIS-I	-233.5874344608287
ACIS-S	-190.1400660498719
HRC-I	126.9829799899862
HRC-S	250.4660330802010

Table 2: Offset Corrections for *dmcoords* transfer from HRC-I

Transfer	Chip	Median	Mean	σ
HRC-I to HRC-S	ΔX	30.2124	30.1071	3.7514
	ΔY	-20.3101	-21.3574	7.0551
HRC-I to ACIS-I	ΔX	-4.6525	-4.6963	2.0368
	ΔY	-5.0700	-6.4540	3.8204
HRC-I to ACIS-S	ΔX	1.8475	2.7629	2.8904
	ΔY	-3.9200	-4.2233	1.4864

6   Optical Axis and Aimpoint positions

Combining the results from Sections 3–5, we can have pictures of optical axis and aimpoint positions in chip coordinates on all four detectors. Figure 17 shows these four pictures for the four detectors. The red arrows show the aimpoint position drift on each detector, data are taken from the median aimpoints in 6 months bins shown in Figures 2–5. Blue diamonds show the optical axis positions on each detector, described in Sections 4 and 5.

During the course of past 12 years of Chandra operation, the optical axis position has been relatively stable. The movement is well within a $10''$ region. The aimpoint, however, has been drifting towards the SIM $[-Y,-Z]$ direction since launch until early 2011, for about $25''$. Since early 2011, it has started to drift back, especially after the safemode in July 2011. In October 2011, the aimpoint has drifted back to near its year 2007 position.

The relative position between the optical axis and aimpoint is changing due to the aimpoint drift. But at no time these two were more than $20''$ apart, which is very small and doesn't cause any concern about degradation of the PSF. Currently (November 2011), the distance between the optical axis and aimpoint is about $12''$.

Figure 18 is the same as Figure 17 but also shows all the individual aimpoints from all the observations with the nominal SIM-Z position.

Figure 19 is the same as Figure 18 but shows all the aimpoints after the safemode as cyan +'s. It is seen that the aimpoint position fluctuates in wide range after the safemode.

7   Default offsets

To avoid the aimpoint getting too close to the chip edge or node boundary so that the dither pattern[1] falling off the chip or crossing the node, default pointing offsets were applied. Since the aimpoint has been drifting, the default offset has been adjusted accordingly during the course of Chandra operation.

ACIS-I: At the launch, there was no need to set default offset since the aimpoint on ACIS-I is well within the chip and far enough from the chip edge. Thus there was no default offset until December 2006, when the aimpoint made a large shift after the ACA cooldown. Since then, default Y-offset$=-12''$ & Z-offset$=-15''$ were applied to all the ACIS-I observations.

ACIS-S: At the launch, the aimpoint was near the node 0|1 boundary. So a default Y-offset$=-20''$ was applied to move the aimpoint away from the node boundary. However, the aimpoint had been drifting into node 0, thus bring the default aimpoint closer and closer to the node

---

[1]Dither is a Lissajous figure, with a peak-to-peak span of $16''$ on ACIS and $40''$ on HRC.

boundary again. In December 2005, the aimpoint had drafted far enough so a new Y-offset=$10''$ was applied to move the aimpoint away from the node boundary to the other direction. In December 2006 after the ACA cooldown, the aimpoint shifted far enough from the node boundary so that Y-offset is no longer needed. Instead, a Z-offset=$-15''$ is applied to bring the aimpoint closer to the optical axis. This default offset lasted until July 2011, when two observations had the dither pattern crossed node boundary again after the safemode. In August 2011, a new Y-offset=$+9''$ was added to the Z-offset=$-15''$ default offset.

In Figures 17–19, green arrows on ACIS-I and ACIS-S indicate these default offsets applied since Chandra launch to compensate the aimpoint drift. Table 3 summarizes these default offsets.

Table 3: Default Offset on ACIS

Detector	Date Applied	Y-offset	Z-offset	Note
ACIS-I	1999 Aug.	0.0	0.0	No offset needed
	2006 Dec.	$-12''$	$-15''$	Move the aimpoint away from the I3 edge
				& closer to optical axis.
ACIS-S	1999 Aug.	$-20''$	0.0	Move the aimpoint away from node 0|1
	2005 Dec.	$+10''$	0.0	Move the aimpoint away from node 0|1
	2006 Dec.	0.0	$-15''$	Move the aimpoint closer to optical axis.
	2011 Aug.	$+9''$	$-15''$	Move the aimpoint away from node 0|1
				& closer to the optical axis.

The aimpoints on HRC-I and HRC-S are well within the center region of both detectors. Thus there are no default offset ever needed for HRCs.

8 Current Optical Axis and Aimpoint positions

Each October, a table of Current Optical Axis and Aimpoint positions are compiled for the new release of Chandra POG (Proposers' Observatory Guide), CIAO (Chandra Interactive Analysis of Observations) and ObsVis (The Chandra Observation Visualizer). The Current Optical Axis and Aimpoint positions released in October 2011 for Chandra cycle 14 are shown in Table 4

Table 4: Chandra Optical Axis and Aimpoint Positions (2011)

Detector	SIM-Z (mm)	Optical Axis ChipX	ChipY	Aimpoint ChipX	ChipY	Chip	Default offset
ACIS-I	-233.587	970	978	945	983	I3	none
				976	959	I3	$\Delta Y=-12''$ & $\Delta Z=-15''$
ACIS-S	-190.143	234	518	227	491	S3	none
				209	521	S3	$\Delta Y=+9''$ & $\Delta Z=-15''$
HRC-I	126.983	7586	7738	7632	7798		none
HRC-S	250.466	2197	8912	2107	8948	S2	none

9   Discussion

In this section, we discuss the possible cause of the observed drift of the aimpoint and optical axis. Figure 20 shows the Chandra Fiducial Transfer System, which illustrate the target acquisition process. First the ACA is pointed to the target. The HRMA, which is (almost) parallel the the ACA, is then also pointed to the target. The SIM is connected to the HRMA by a Optical Bench Assembly (OBA). A set of fiducial LED lights surrounding each detector is fed through a retroreflector collimator mounted in the HRMA then onto the ACA CCD, to register the SI focal plane laterally wrt the ACA boresight. This information is saved in the *asol* file accompanying the observing data file.

There are two possible causes for the drift: 1) the SIM is shifted wrt the HRMA due to the bending of OBA or relative shift between the SIM and the OBA; 2) the alignment change between the ACA and the HRMA.

If it were due to the first cause, both optical axis and aimpoint would have drifted the same way. The fact that the optical axis has been relatively stable in the past 12 years indicates that the relative position between the SIM and the HRMA, and therefore the OBA, are pretty rigid and stable. So we can rule out the first possible cause.

The second cause would make the aimpoint drift, since it would change the pointing alignment between the ACA and the HRMA. But it would have no effect on the optical axis. This is exact what we observed. This cause is further confirmed by the fact that a sudden change in the ACA housing temperature, e.g. the ACA cooldown or safemode, can cause a rather large shift of the aimpoint position.

Therefore we conclude that the reason causing the aimpoint to drift is the alignment change between the ACA and the HRMA. This alignment change can also be divided into long term change and short term change. The long term change may be due to the aging and relaxing of the material, which is beyond our control. The short term change is usually associated with the thermal change in the ACA housing. So the key to keep the aimpoint stable in a short term is to keep a constant temperature of the ACA.

References

[1] Zhao, Ping, "Chandra Telescope Optical Axis and Aimpoint", 2006, CXC Memorandum, http://cxc.harvard.edu/cal/Hrma/rsrc/Public/OpticalAxisAndAimpoint/opt_axis_memo.pdf

# Chandra Detectors Layout − SIM Translation Table
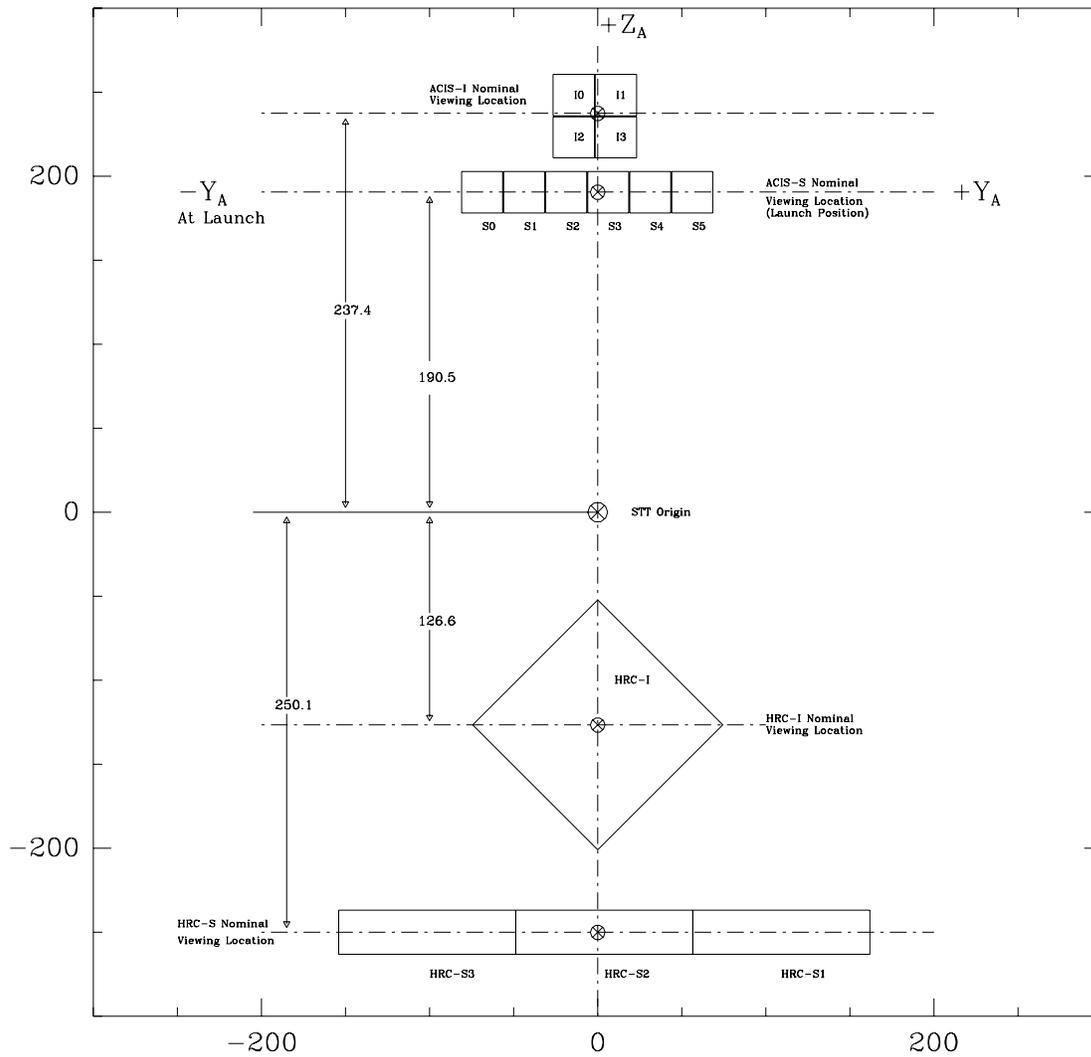
Figure 1: Chandra Detectors Layout: The SIM Translation Table shows the flight focal plane instrument to scale (in mm, coordinate system is AXAF-STT-1.0). SIM +Y is in x-axis; SIM +Z is in y-axis. ⊗ on each detector marks the aimpoint position with zero pointing offset.
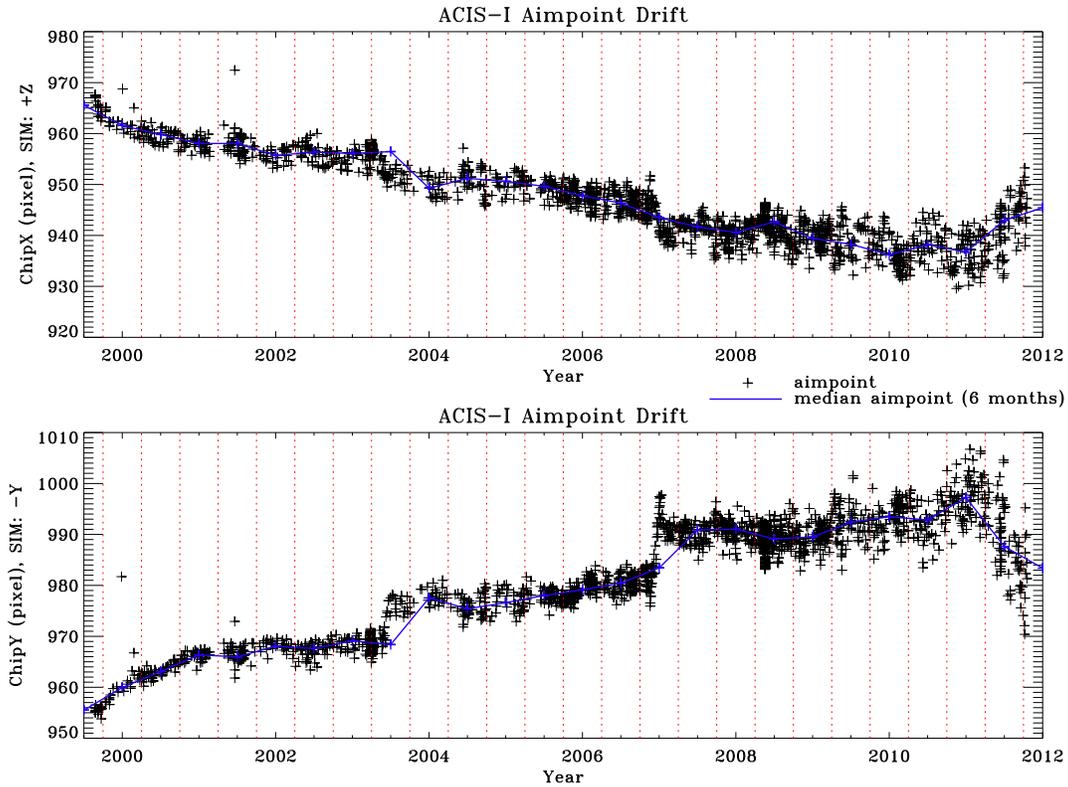
Figure 2: ACIS-I aimpoint position as a function of time. Solid blue line shows the drift of median aimpoint in 6 months bins, which are separated by vertical dotted red lines.
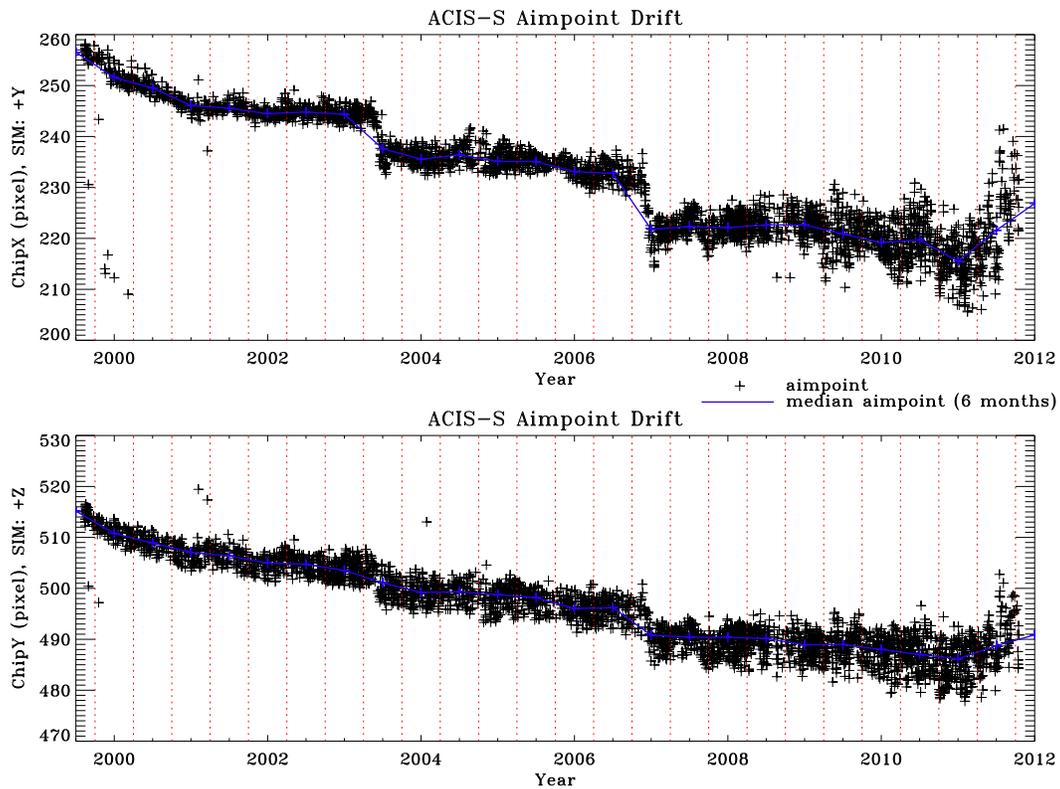
Figure 3: ACIS-S aimpoint position as a function of time. Solid blue line shows the drift of median aimpoint in 6 months bins, which are separated by vertical dotted red lines.
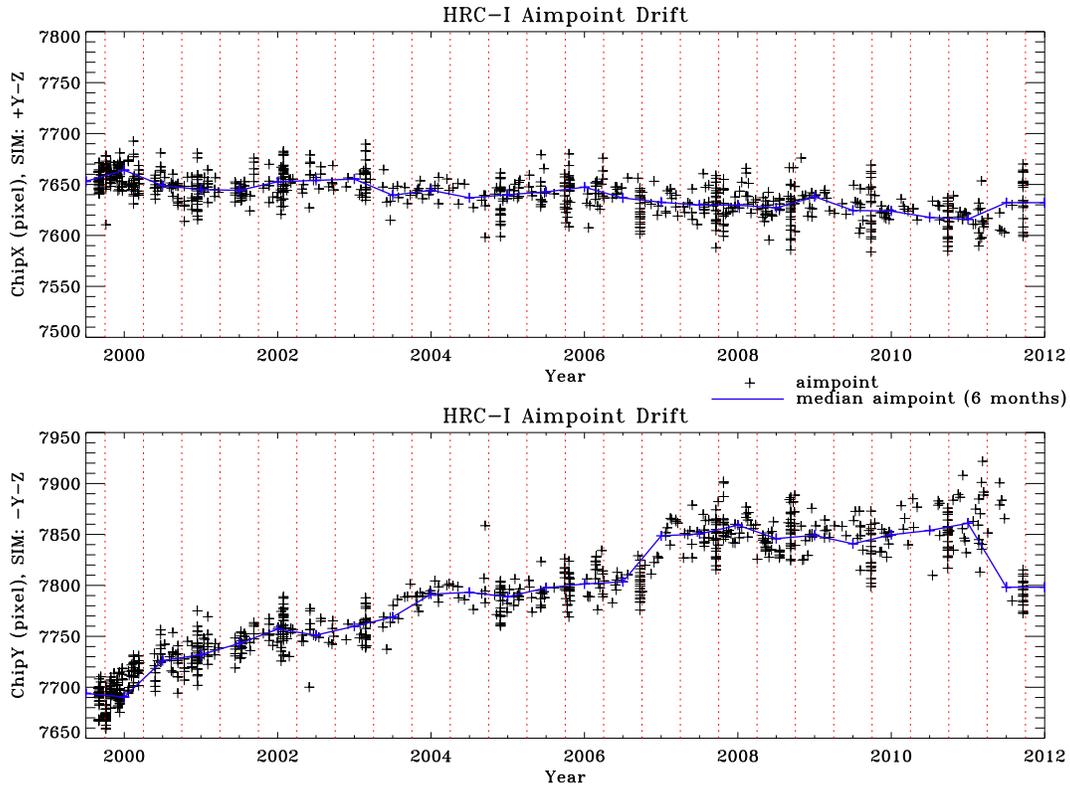
Figure 4: HRC-I aimpoint position as a function of time. Solid blue line shows the drift of median aimpoint in 6 months bins, which are separated by vertical dotted red lines.
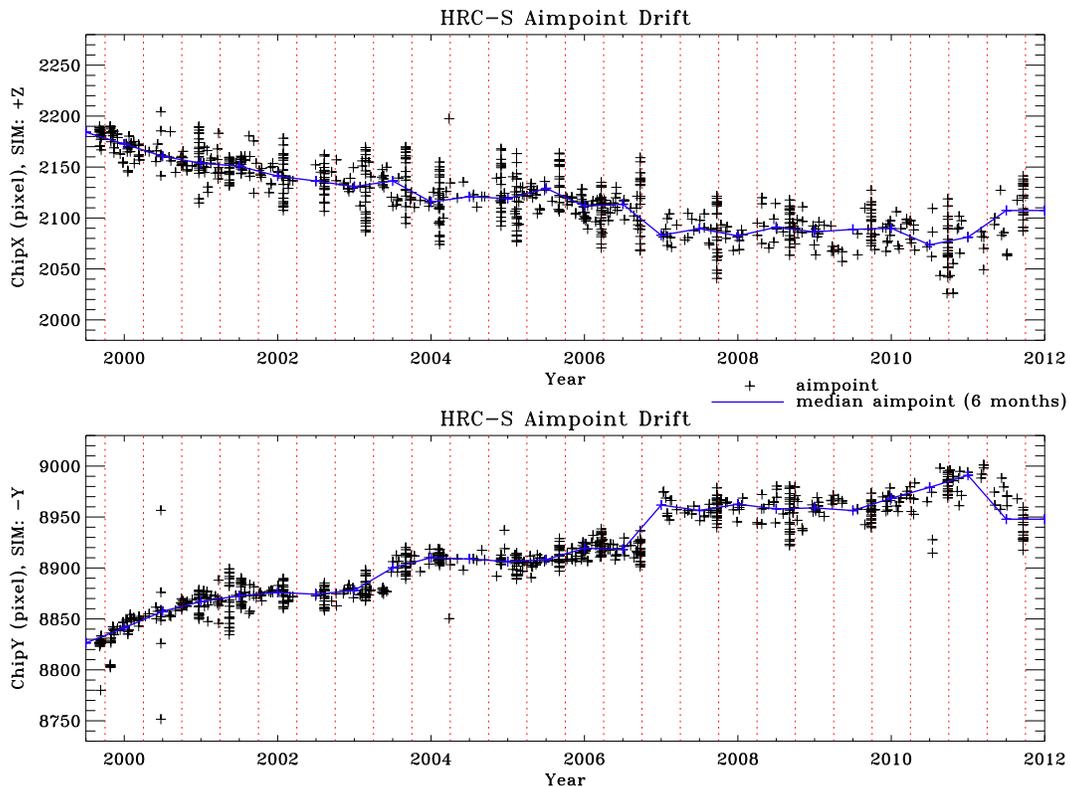
Figure 5: HRC-S aimpoint position as a function of time. Solid blue line shows the drift of median aimpoint in 6 months bins, which are separated by vertical dotted red lines.
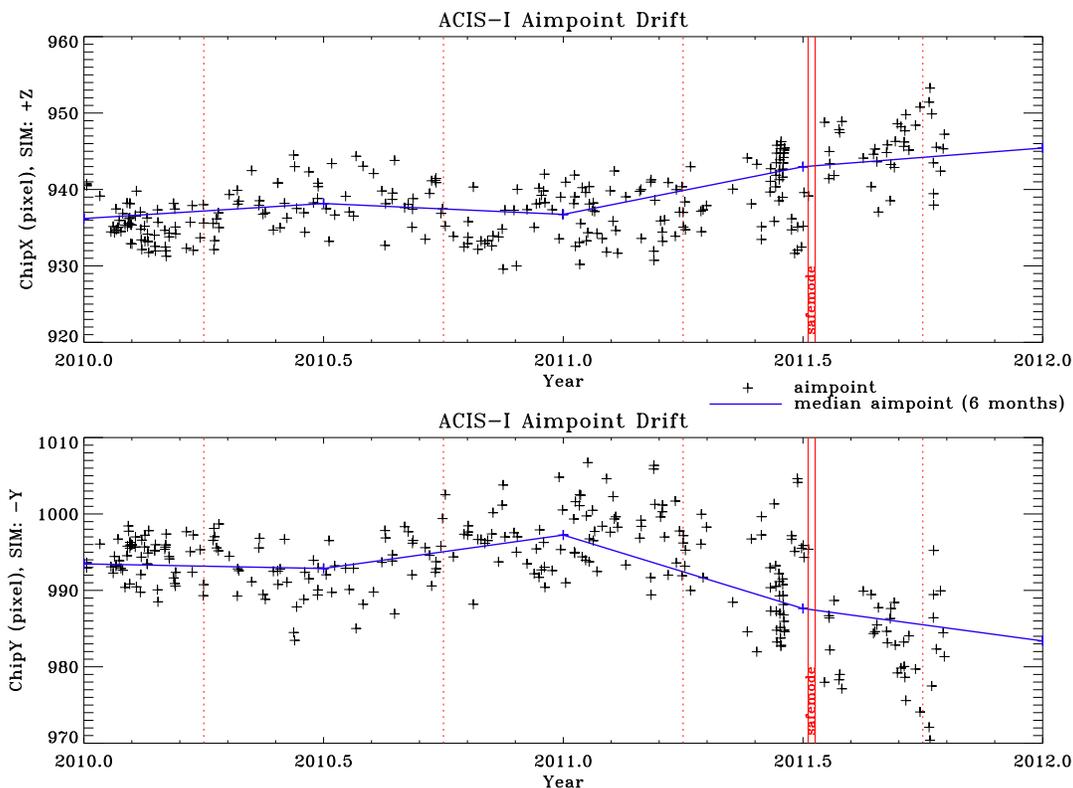
Figure 6: ACIS-I aimpoint positions since Jan. 1, 2010. Vertical solid red lines indicate the gap of safemode in July 2011.
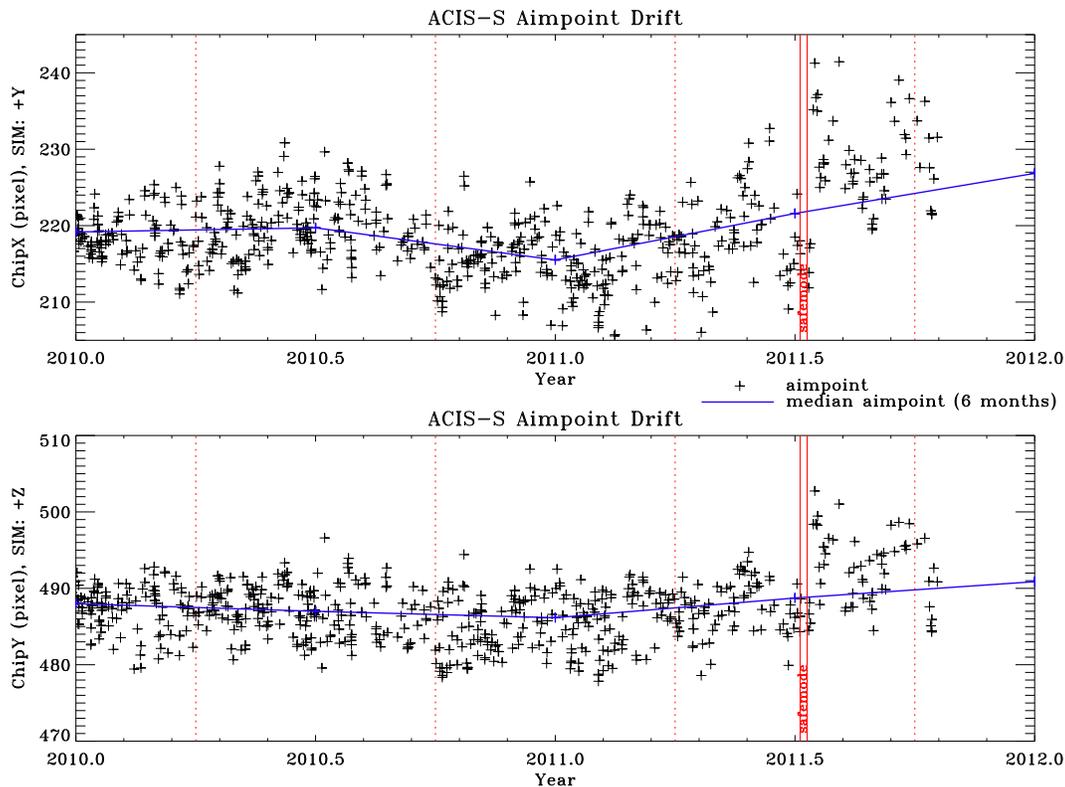
Figure 7: ACIS-S aimpoint positions since Jan. 1, 2010. Vertical solid red lines indicate the gap of safemode in July 2011.
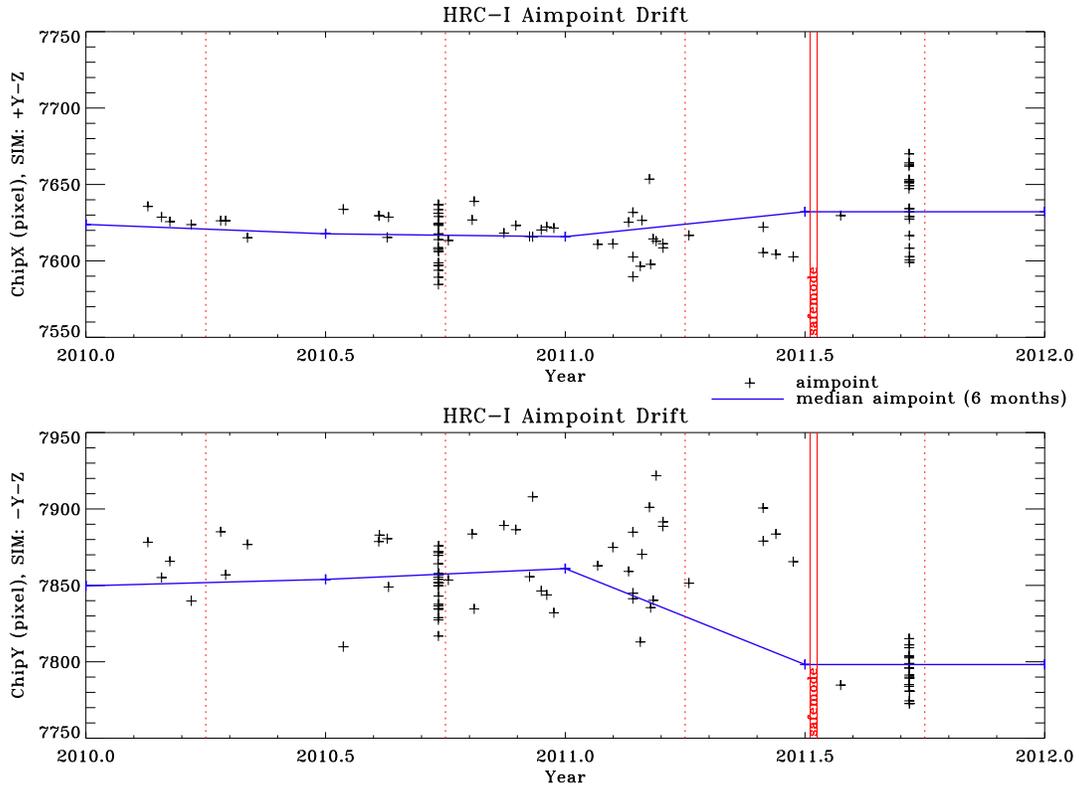
Figure 8: HRC-I aimpoint positions since Jan. 1, 2010. Vertical solid red lines indicate the gap of safemode in July 2011.
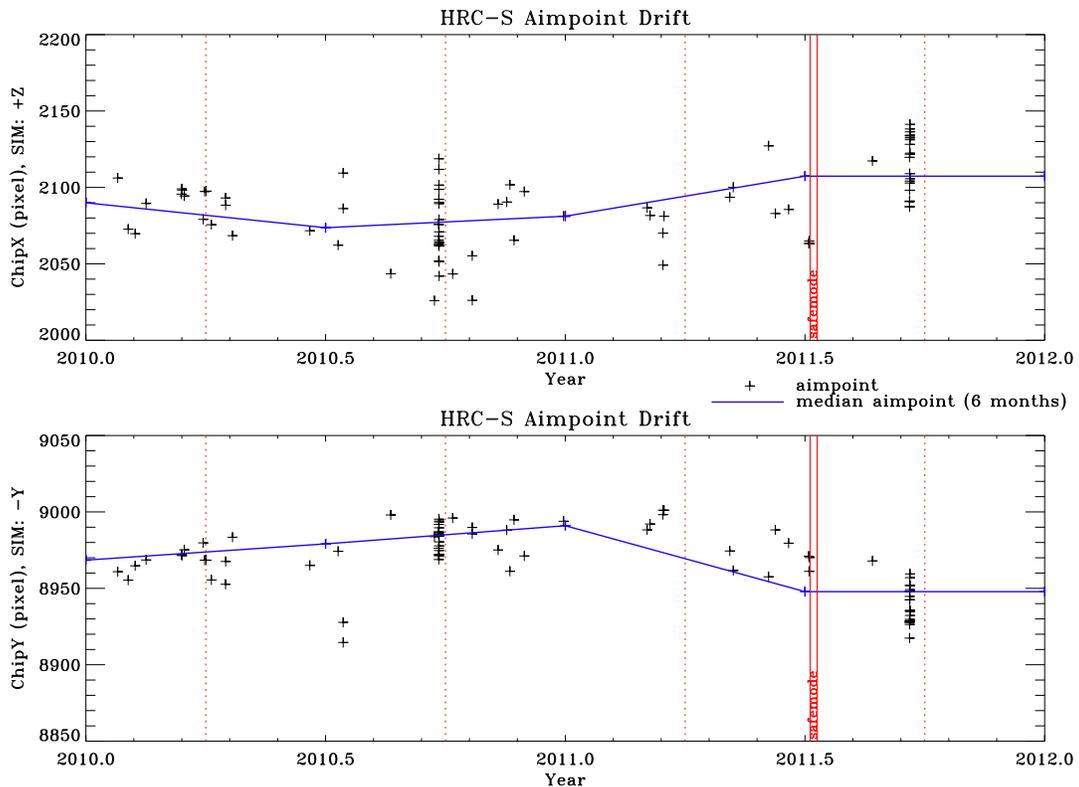
Figure 9: HRC-S aimpoint positions since Jan. 1, 2010. Vertical solid red lines indicate the gap of safemode in July 2011.
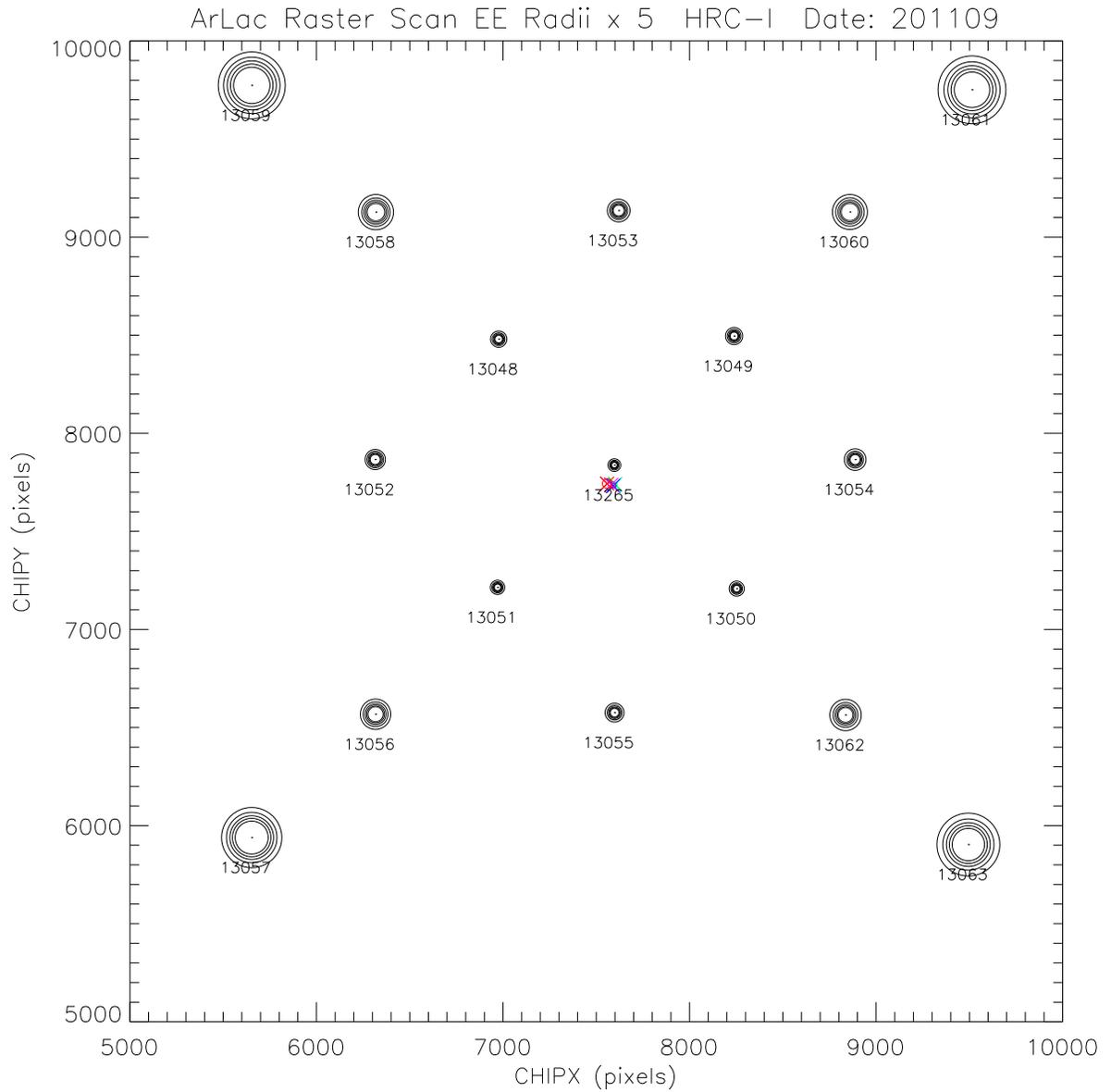
Figure 10: HRC-I raster scan observation of Ar Lac in chip coordinates. Circles around each observation point have the 50% – 90% encircled energy radii × 5. The data are fit to a 2-D quadratic function to find the optical axis. Data taken in September 2011.

ArLac Raster Scan EE Radii   HRC−I   Date: 201109

× Optical Axis: (7585.57±17.1, 7738.24±4.07)
+ Centroid: (7596.68,7837.87), d=13.20", α=51.363°

× 50% EE: (x0,y0,r0)=(7600.9, 7740.6, 1.849)
× 60% EE: (x0,y0,r0)=(7597.6, 7736.8, 2.222)
× 70% EE: (x0,y0,r0)=(7590.5, 7732.7, 2.775)
× 80% EE: (x0,y0,r0)=(7580.5, 7737.5, 3.578)
× 90% EE: (x0,y0,r0)=(7558.2, 7743.5, 4.928)
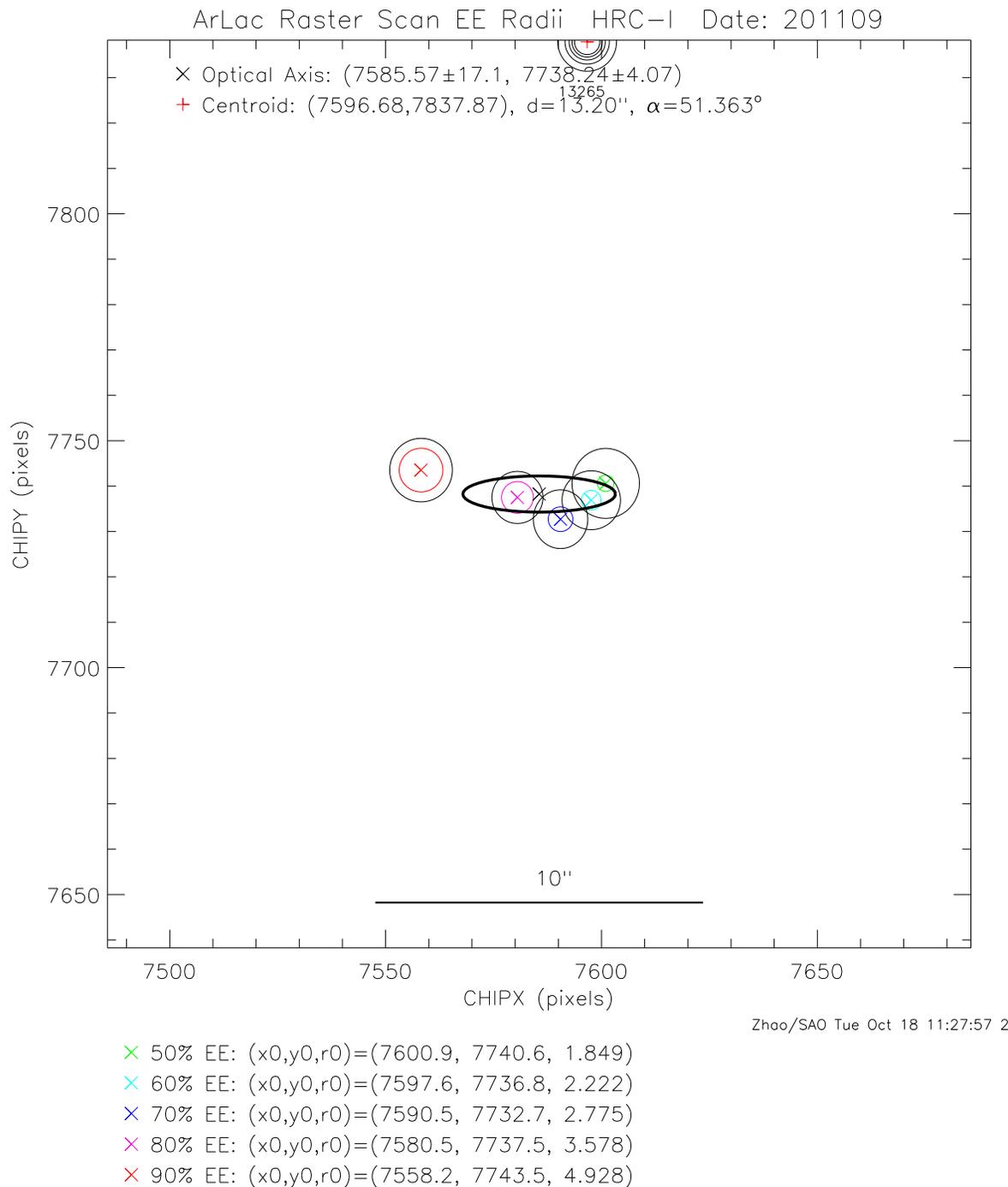
Figure 11: Same as Fig. 10 but zoomed in to the optical axis region. The five colored ×'s are the positions of quadratic function minimum for 50% − 90% EE fit. The colored circles indicate their encircled energy radii. The black circles are the $1-\sigma$ fit errors. The black × marks the optical axis position, taken as the mean of the above 5 minimums. The black oval is the $1-\sigma$ error ellipse.
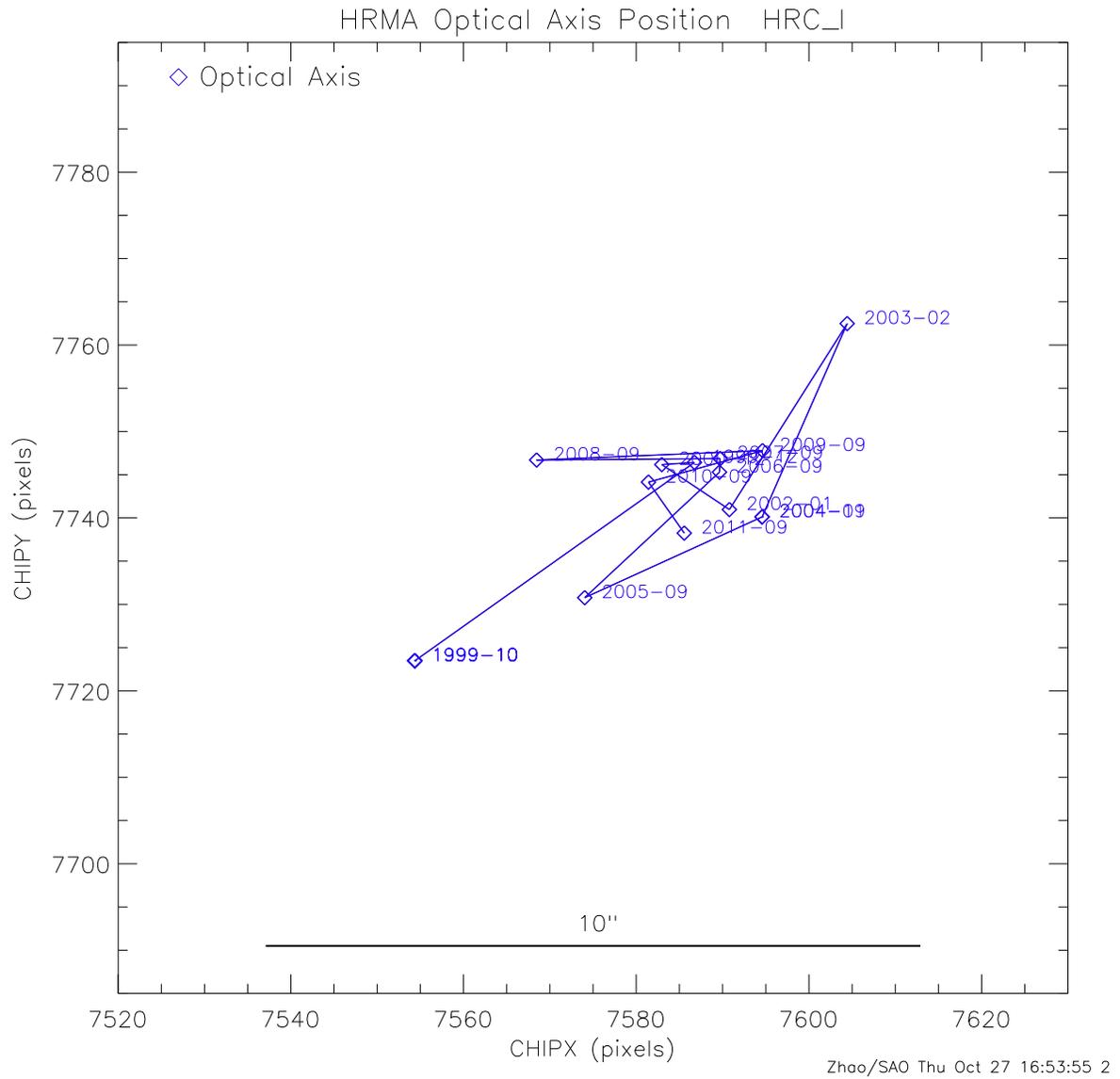
Figure 12: Chandra optical axis positions on HRC-I since launch, labeled by year–month. It is relatively stable and well with in 10″ region.
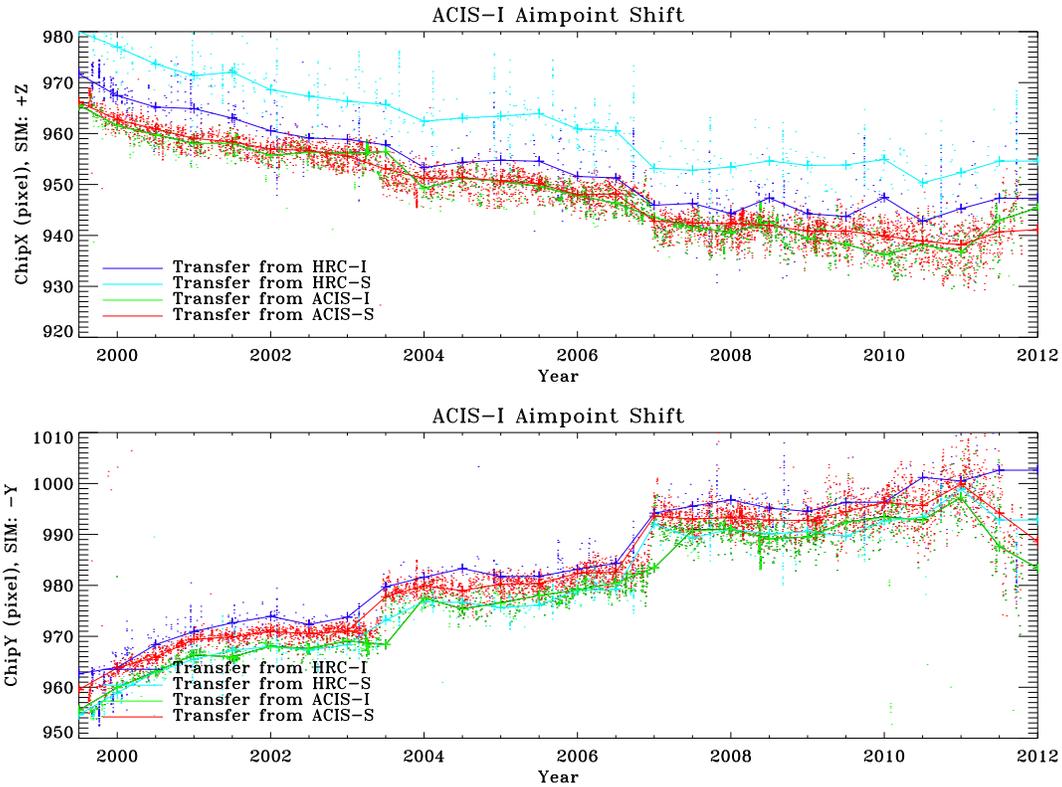
Figure 13: Aimpoints transferred from all detectors to ACIS-I, using *dmcoords*. The four colored solid lines shows the drift of median aimpoint in 6 months bins on four detectors.
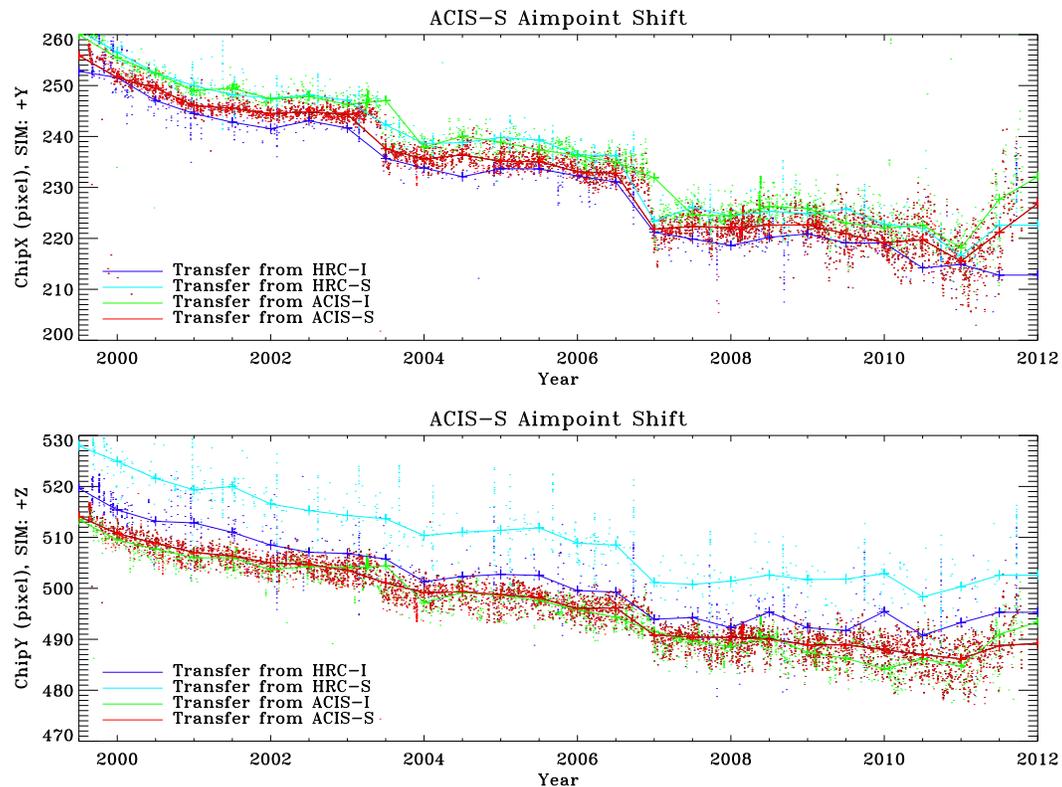

Figure 14: Aimpoints transferred from all detectors to ACIS-S, using *dmcoords*. The four colored solid lines shows the drift of median aimpoint in 6 months bins on four detectors.
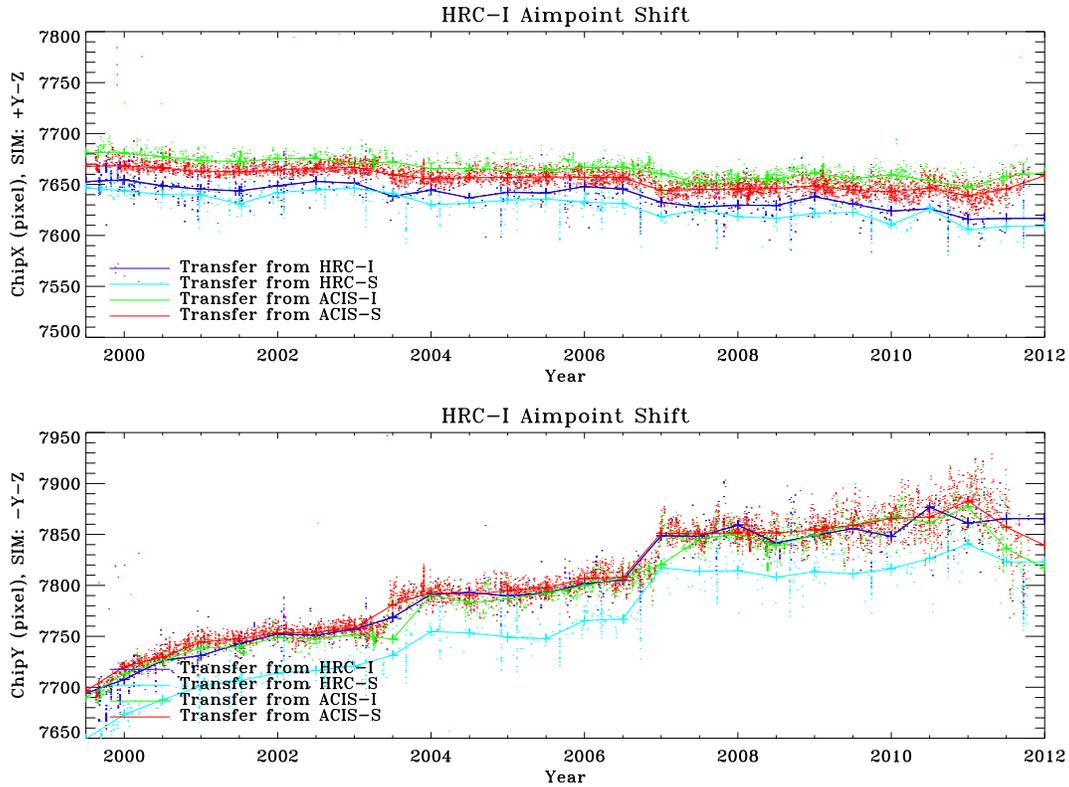
Figure 15: Aimpoints transferred from all detectors to HRC-I, using *dmcoords*. The four colored solid lines shows the drift of median aimpoint in 6 months bins on four detectors.
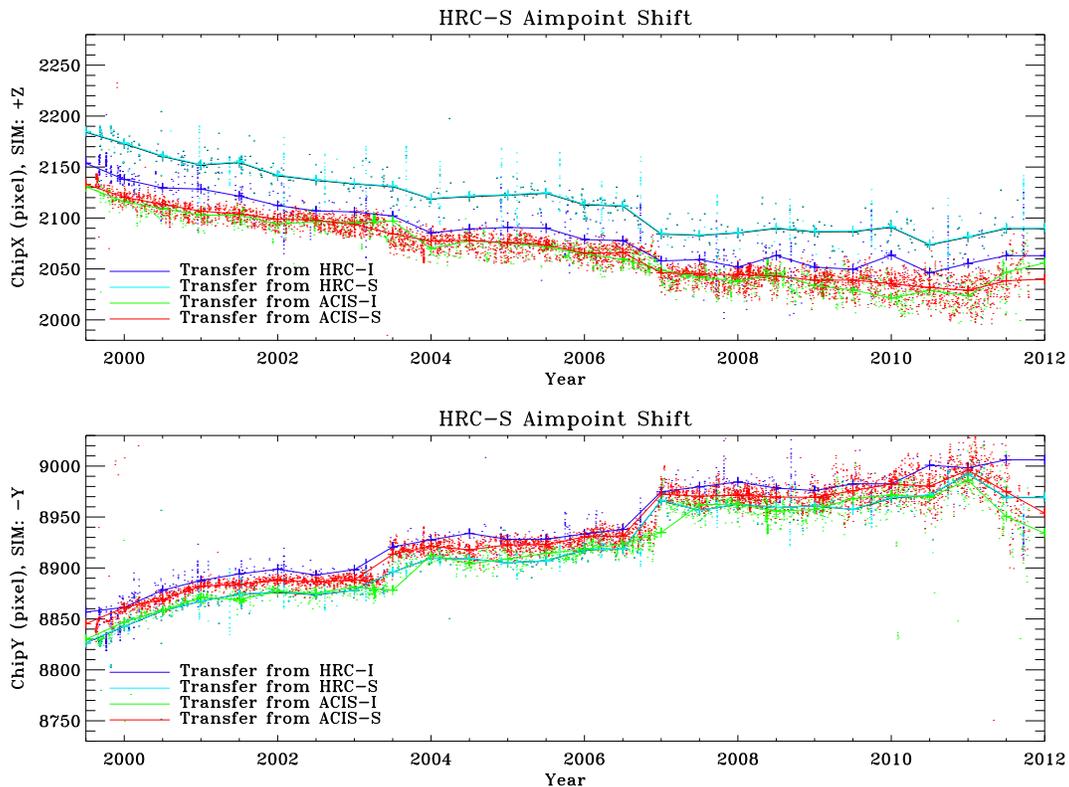
Figure 16: Aimpoints transferred from all detectors to HRC-S, using *dmcoords*. The four colored solid lines shows the drift of median aimpoint in 6 months bins on four detectors.

# Optical Axis and Aimpoint positions, and Default Offsets
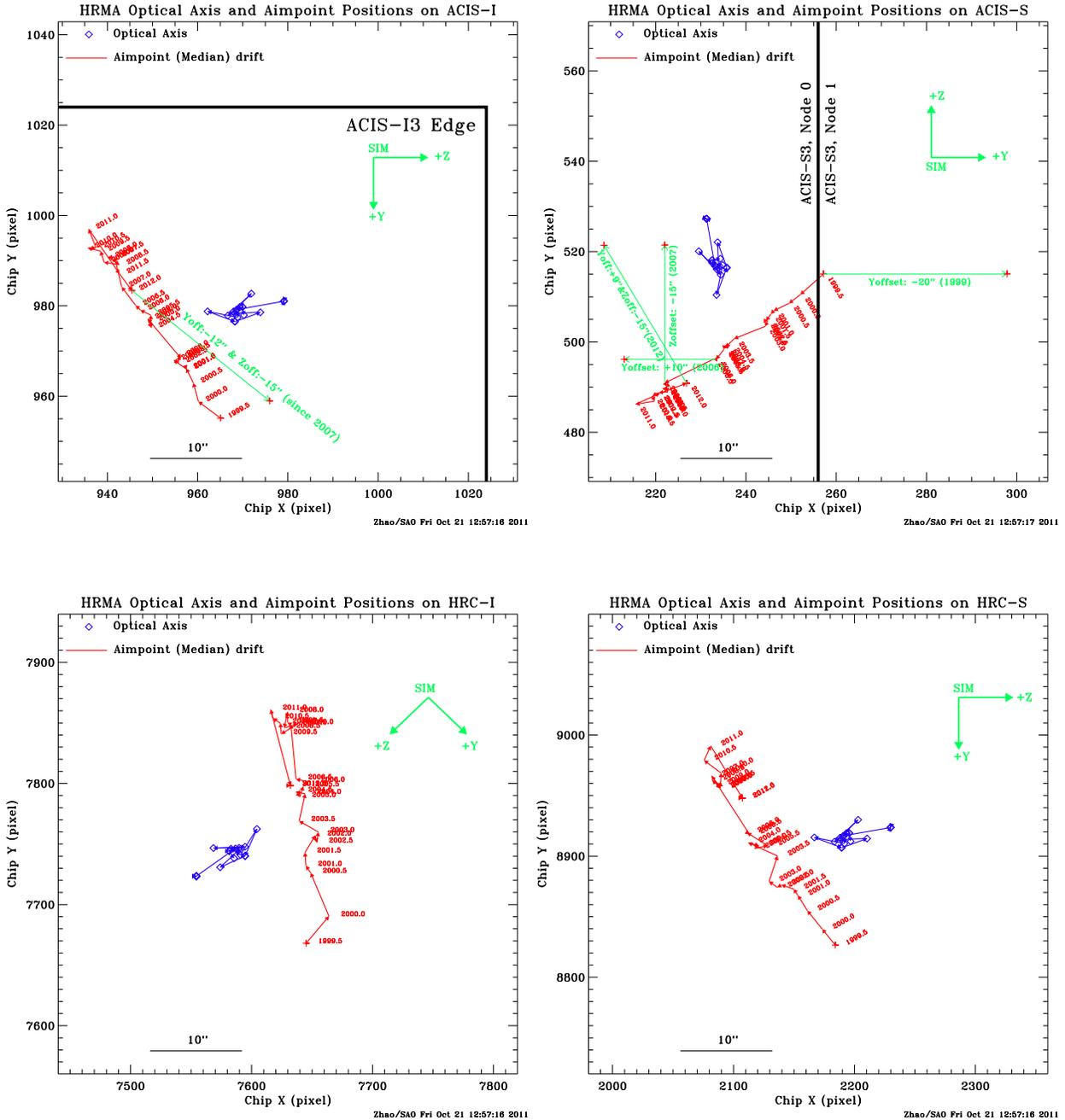
Figure 17: Median aimpoint (red) and optical axis (blue) drifts on ACIS-I (UL), ACIS-S (UR), HRC-I (LL) and HRC-S (LR). While the optical axis are relatively stable, aimpoint has been drifting towards the SIM [-Y,-Z] direction since launch until early 2011. Since then, it started to drift back, especially after the safemode. In October 2011, the aimpoint has drifted back to near its year 2007 position. Green arrows on ACIS-I and ACIS-S indicate the default offsets over the years to compensate the aimpoint drift to avoid the dither pattern of the aimpoint falling off the chip or crossing the node boundary 0|1.

Optical Axis and Aimpoint positions, and Default Offsets
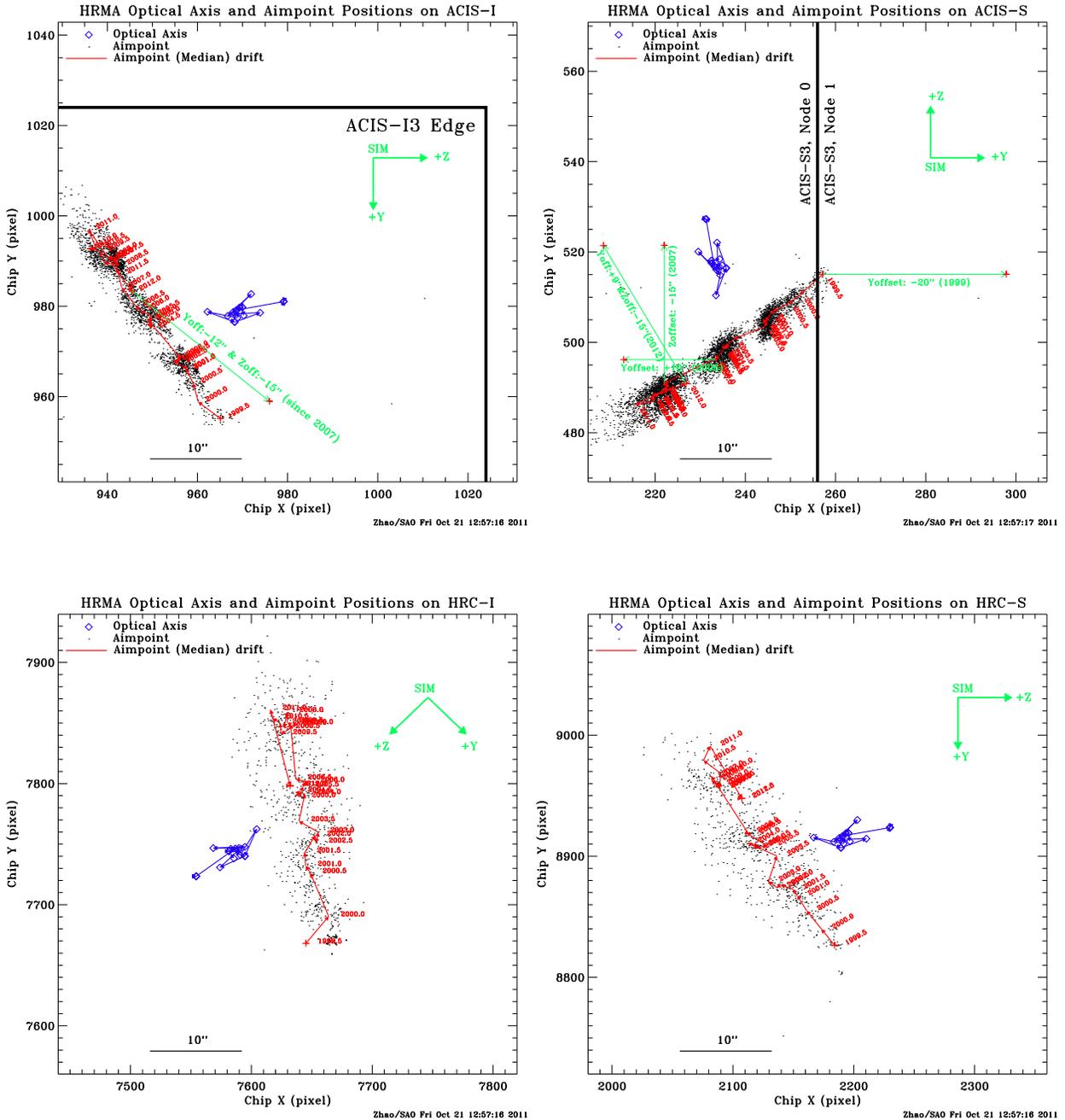

Figure 18: Same as Figure 17, with the aimpoints of individual observations shown as black dot.

# Optical Axis and Aimpoint positions, and Default Offsets
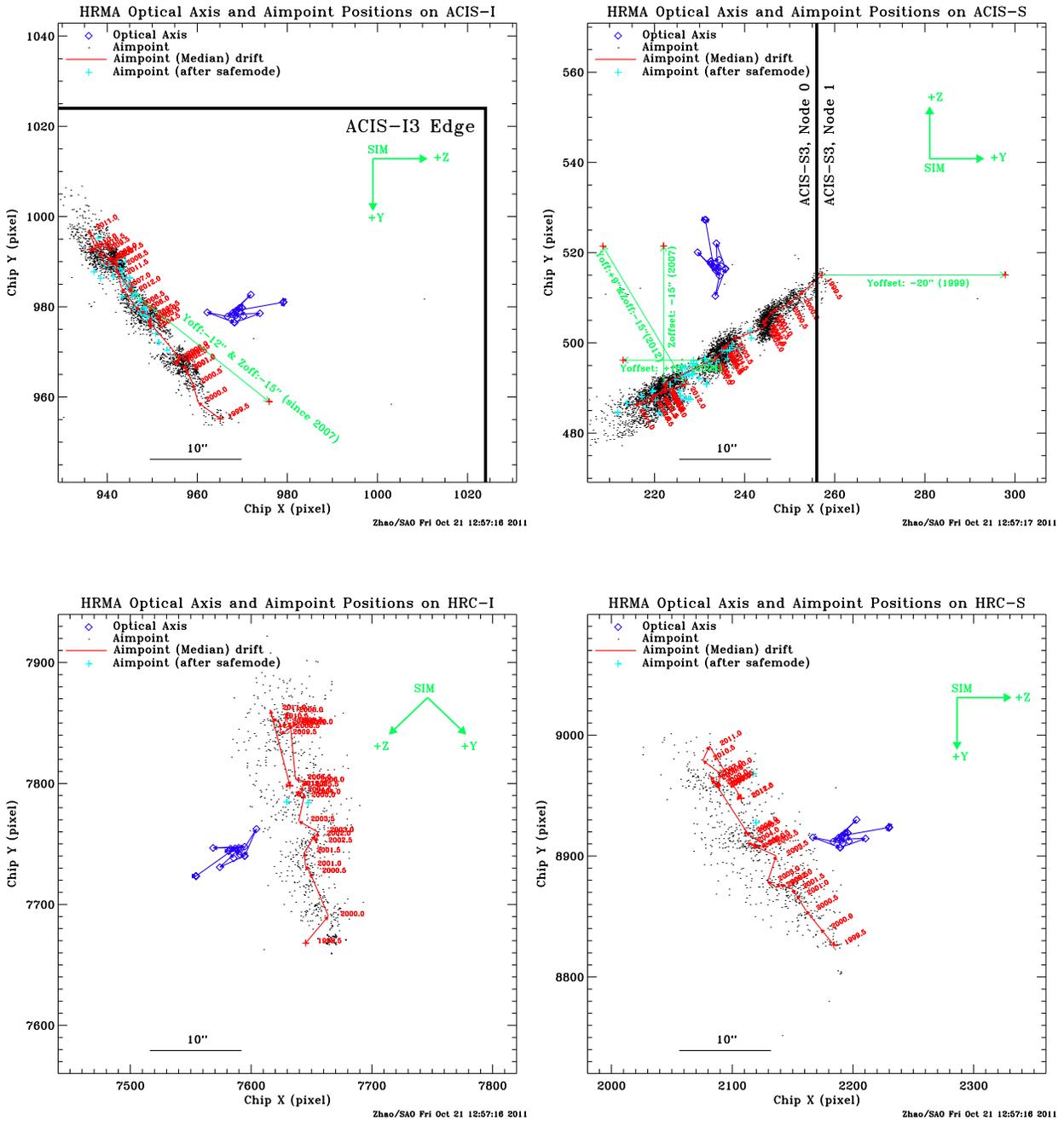
Figure 19: Same as Figure 18, with the aimpoints of individual observations after the safemode shown as cyan "+".

Fiducial lights and Fiducial Transfer System
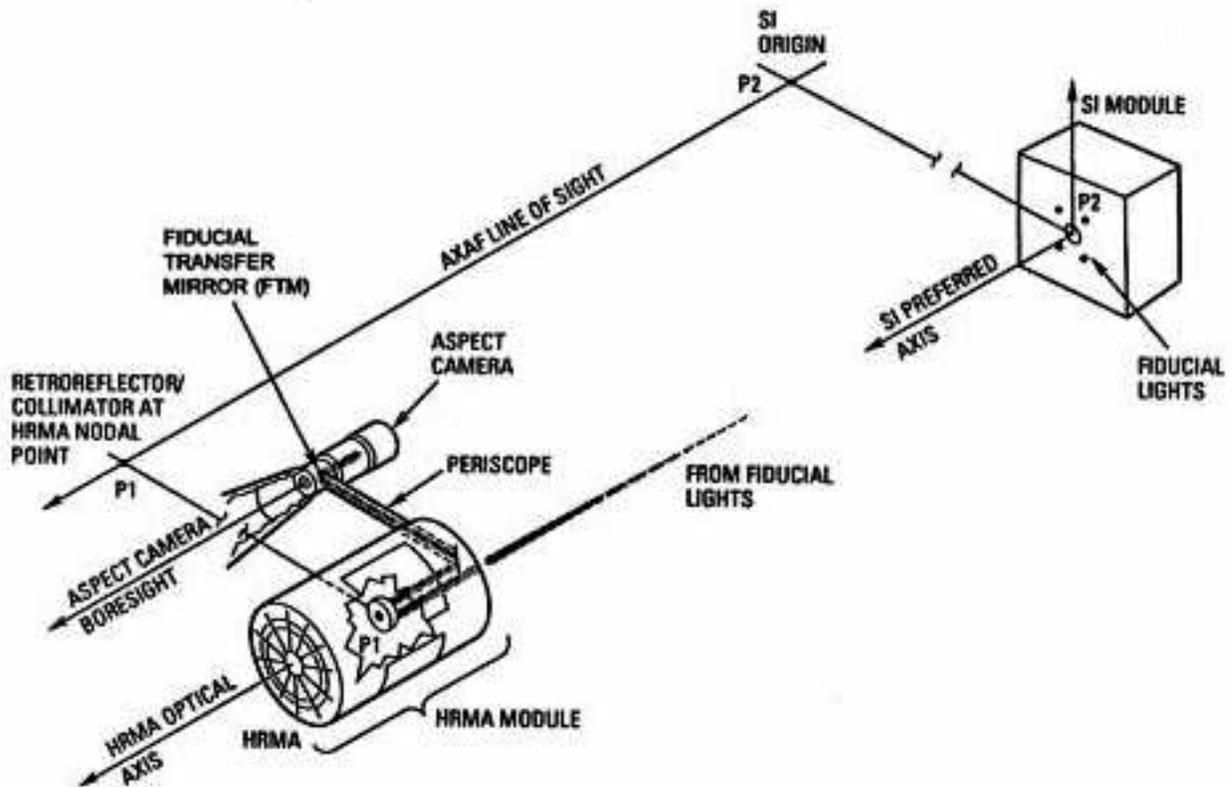
Figure 20: Surrounding each of the SI detectors is a set of light emitting diodes, or "fiducial lights", which serve to register the SI focal plane laterally with respect to the ACA boresight. Each fiducial light produces a collimated beam at 635 nm which is imaged onto the ACA CCD via the RRC, the periscope, and the fiducial transfer mirror. (POG-13, Fig 5.3)